Flame Acceleration and Defagration-to-Detonation Transition through an Array of Obstacles

Huahua Xiao, Ryan W. Houim, Elaine S. Oran
Department of Aerospace Engineering
University of Maryland
College Park, Maryland, 20742, USA

1 Introduction

Obstacle-laden channels are often used to study flame acceleration and deflagration-to-detonation transition (DDT) in a controlled manner [1-8]. Common applications are for evaluating the likelihood of a detonation for ensuring safety and development of detonation-based engines. The basic mechanisms underlying flame and flow acceleration in channels with orifice plates or fence-type obstacles aligned with channel walls involve thermal expansion of hot combustion products, flame-vortex and acoustic-shock-flame interactions, and Rayleigh-Taylor (RT), Richtmyer-Meshkov (RM) and Kelvin-Helmholtz (KH) instabilities. These phenomena lead to a turbulent flame, which further accelerates the flow. The accelerating flow generates strong shocks and create conditions at which flames accelerate quickly and DDT can occur. Detonations can be triggered in the vicinity of turbulent flames through Zeldovich's reactivity-gradient mechanism once hot spots are created by Mach-stem reflections from obstacles [1, 4, 6]. Another mechanism is *shock focusing*, which occurs when enough energy is deposited in a small location to initiate a detonation directly [9-11].

The configuration or layout of obstacles has a significant effect on the flame acceleration and DDT [12-16]. Practical applications may involve an array of obstacles, such as cooling pipes in power plants, pipes in chemical processing plant, and vessels in storage facilities. Ogawa et al. studied flame acceleration and DDT in an unconfined, obstructed containing an array of square [14] or cylindrical [13, 17] obstacles. It was found that in the initial stages, the flame accelerates faster in the directions without flow obstruction. As shock waves build up, however, shock-flame interactions become extremely important in the flow, the flame accelerates faster, and DDT occurs in more obstructed directions through the hot-spot mechanism. The reaction waves propagate as quasi-detonations at the final stage. For the cylindrical array, DDT could not occur when the obstacles are aligned parallel to the direction of flame propagation. Pinos and Ciccarelli [12] conducted experiments of combustion wave propagation in a channel with a bank of cylinders, and found that initial flame acceleration is greatly influenced by the blockage ratio rather than the obstacle layout. They discussed detonation ignition and development of quasi-detonation propagation, mode. Unfortunately, however, the initial DDT event was not captured in the experimental photographs.

Correspondence to: Huahua Xiao, hhxiao@umd.edu

In this work, we solve the unsteady fully compressible computational fluid dynamics equations with adaptive mesh refinement (AMR) to study flame acceleration and DDT in a channel with an array of cylindrical obstacles. These results are then described and comparisons are made to previous experiments [12]. In addition, the effect of the shape of obstacles is examined.

2 Physical and Numerical Models

The numerical simulations solve the two-dimensional (2D) fully compressible Navier-Stokes equations with a model of chemically reacting stoichiometric hydrogen-air mixture. Details of the governing equations are in [18, 19]. The combustion of premixed stoichiometric hydrogen and air at 1 atm and 293 K is modeled by a single-step chemical-diffusive model [6]. The reaction rate is defined as $\dot{\omega} = A\rho Y \exp(E_a/RT)$, where A, ρ, Y, R and E_a are the pre-exponential factor, density, unburned mass fraction, universal gas constant, and activation energy, respectively.

The equations are solved on a dynamically adapting grid [20] using a Godunov algorithm, third-order accurate in space and second-order in time [18]. Figure 1 shows the 2D computational configuration, which describes a 76.4 mm high channel with an array of cylinders. To allow a comparison with experiments, the geometry of the obstructed channel is set to be the same as the inline channel geometry with a blockage ratio of 0.5 in [12]. The obstacles are evenly spaced in both horizontal and vertical directions and are modeled using an immersed boundary method [21]. The obstacle diameter is 12.7 mm. The minimum grid size is 37.3 μm, corresponding to 10 computational cells in the flame under initial conditions. The numerical resolution test showed that the cell size is adequate. The flame was ignited using a semi-circular pocket of hot, burned gas with a radius of 1 mm at the left end on the channel axis.

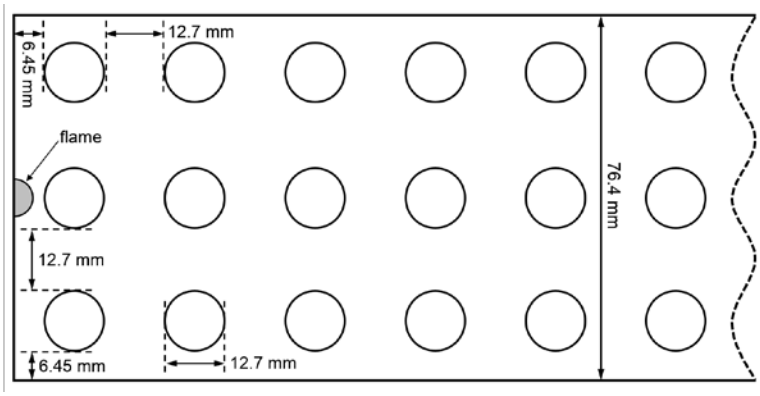

Figure 1. Computational domain of an array of obstacles. No-slip, reflecting and adiabatic boundaries are used for the walls and obstacle surfaces. The radius of the initial flame is 1 mm.

3 Numerical results

Figure 2 compares time sequences of the accelerating flame and flow in the simulation and the experiment [12]. Overall, the flame and flow development agrees well with the experiments. The early flame acceleration results from the rapid expansion of the flame into the background flow and stretching in the wakes of cylinders, as shown in the previous simulations [13, 17] and experiments [12]. After ignition, the flame rounds the obstacles and is elongated in the unobstructed directions, as shown at 1.52 ms. As shock waves are generated by the accelerating flame, more flame instabilities are produced due to flame-shock interactions, such as RM and KH instabilities, as shown at 1.97 ms. This results in a large increase in the

flame surface area and faster flame acceleration. As the flame continues to propagate, it becomes turbulent and produces a strong leading shock, which moves out ahead of the flame, as shown at 2.05 ms.

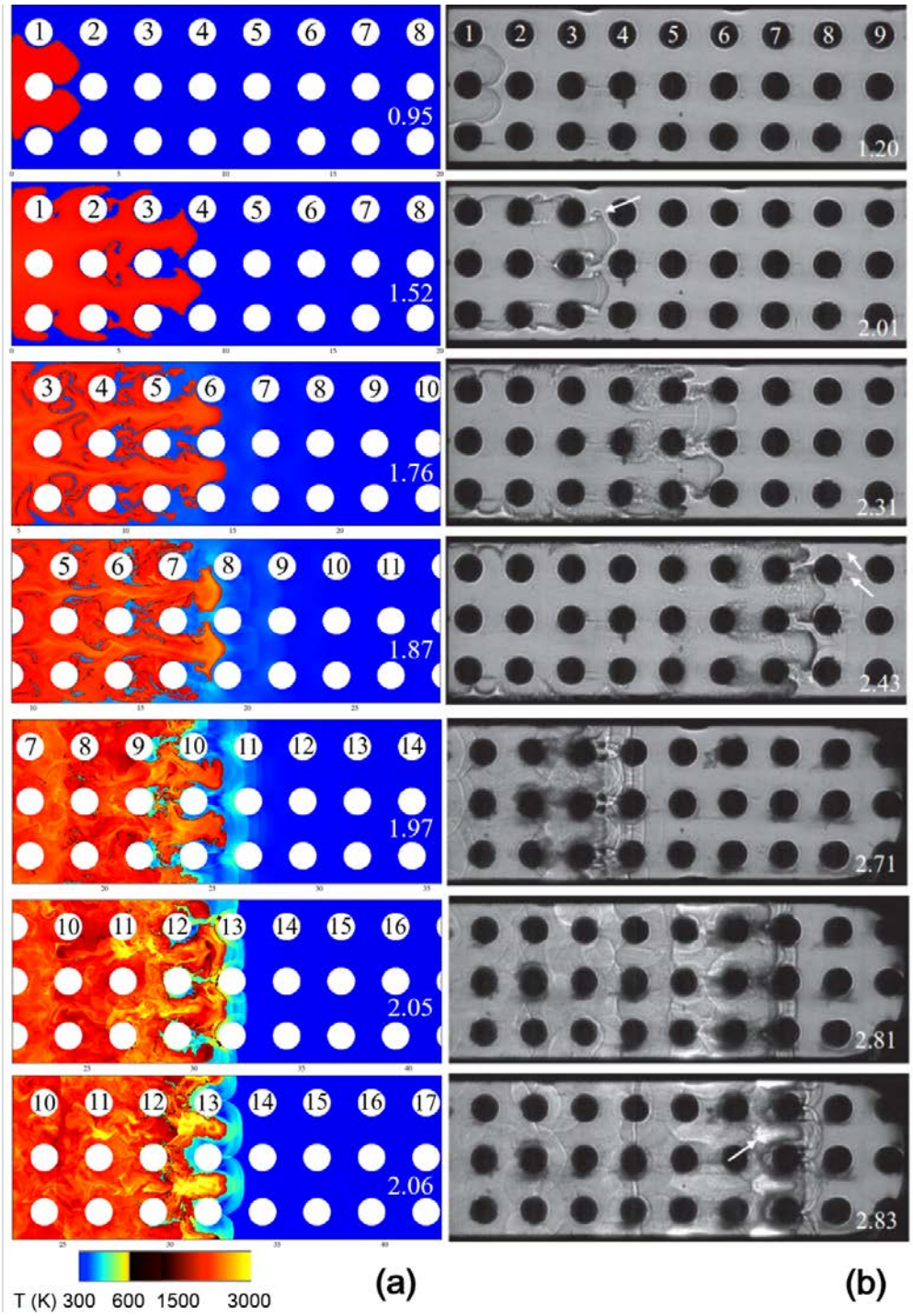

Figure 2. Accelerating flames in a channel with an array of cylinders. (a) Temperature fields in the simulation. (b) Schlieren images in the experiments by Pinos and Ciccarelli [12]. Obstacles are numbered. Time in milliseconds is given in the right-bottom corner in each frame.

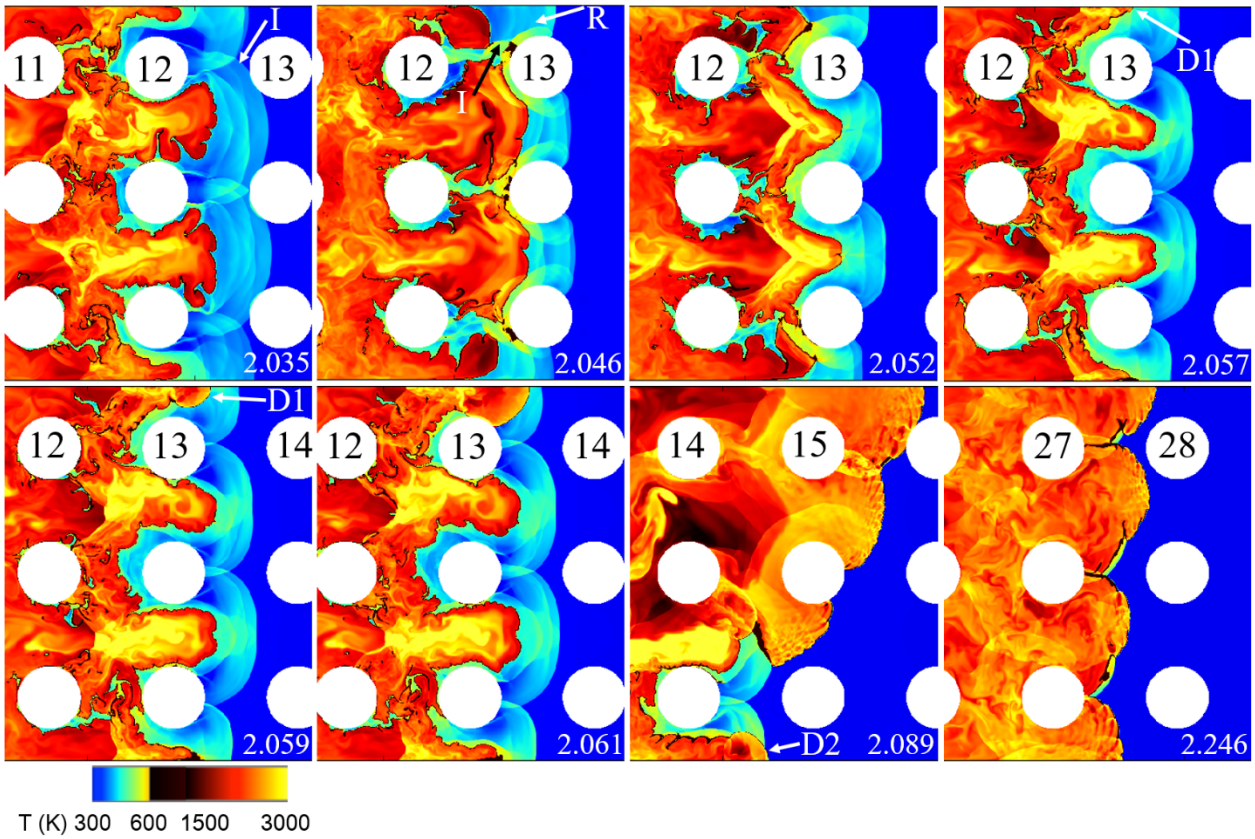

Figure 3. A sequence of temperature maps showing DDT. Times in milliseconds are given at the frame bottom-right corners. I: incident shock; R: reflected shock; D1: first detonation; D2: second detonation.

The flame propagates faster after ignition in the calculation. The possible reason is that three-dimensional expansion and stretch of the initial flame lead to a weaker flame acceleration in the experiment.

Figure 3 shows the computed DDT process from a sequence of temperature fields. As the flame front passes obstacle Row 12, the leading shock reaches Row 13 which is marked as an incident shock I, as shown at 2.035 ms. The incident shock is radially reflected as it passes over the obstacles. In particular, a reflected shock (marked as R) travels toward the upper boundary, as shown at 2.046 ms. This shock appears to be a reflected Mach-stem, but it does not create hot-spot. The incident shock I and the reflected shock form a triple point. When the triple point collides with the upper wall right at the upper flame tip in the shocked region, a detonation (D1) is initiated, as shown at 2.057 and 2.059 ms. The detonation wave soon travels quickly through the unburned mixture. Before this detonation front arrives at the obstacles next to the bottom wall, a second detonation is triggered through the same process as the lower flame tip passes the Row 14, as shown at 2.089 ms. Then the two detonations join together and propagate into the unburned region. The detonation decouples into a flame and shock wave frequently as the detonation front diffracts over the obstacles, as shown in at 2.246 ms.

Here the initiation of detonation involves a collision of shocks in the shocked boundary layers at the flame tips, which appears to be related to mechanism of shocking focusing reported in [10, 11]. Previous work [Refs], using the same inline geometry but with symmetry or periodic upper and lower boundary conditions, could not produce detonation. This, together with the present observation, indicates the importance of boundary layer to the DDT.

Figure 4. shows the computed and measured [12] reaction front speed as a function of the position of the leading reaction-front edge. In the acceleration stage, the flame front speed oscillates approximately as the flame passes over every row of obstacles. While the computed flame-front speed is in very good agreement with experimental result, the accelerating flame in the experiments appears to propagate over a few more rows of obstacles before a detonation was ignited. The detonation failure and re-ignition phenomena observed in the experiments are also reproduced in the numerical simulations.

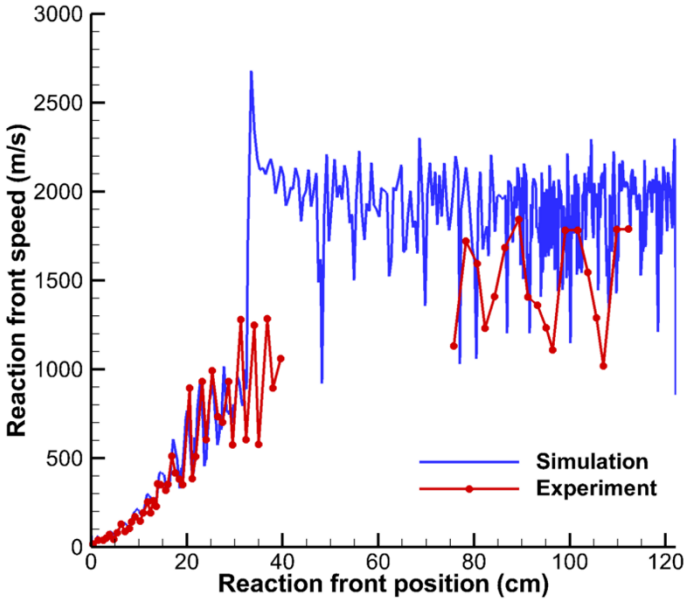

Figure 4. Numerical and experimental [12] reaction-front propagation speed as a function of the location of the leading edge of the reaction front.

The computation described here is only one of a series that we have performed to explore flame acceleration and DDT through an array of obstacles. A more extensive group of computations, which focus on obstacle shapes and blockage ratio, will be discussed in the presentation.

Acknowledgments

This work was supported by the University of Maryland through Minta Martin Endowment Funds in the Department of Aerospace Engineering, and through the Glenn L. Martin Institute Chaired Professorship at the A. James Clark School of Engineering. Parts of the work were funded by the Office of Naval Research Grant No. N00014-14-1-0177. The authors acknowledge the University of Maryland supercomputing resources (http://www.it.umd.edu/hpcc) made available in conducting the research reported in this paper.

References

[1] Kessler DA, Gamezo VN, Oran ES. (2010). Simulations of flame acceleration and deflagration-to-detonation transitions in methane-air systems. Combust. Flame.157: 2063.

[2] Ciccarelli G, Dorofeev S. (2008). Flame acceleration and transition to detonation in ducts. Prog. Energ. Combust. 34: 499.

[3] Oran ES, Gamezo VN. (2007). Origins of the deflagration-to-detonation transition in gas-phase combustion. Combust. Flame. 148: 4.

[4] Gamezo VN, Ogawa T, Oran ES. (2007). Numerical simulations of flame propagation and DDT in obstructed channels filled with hydrogen-air mixture. Proc. Combust. Inst. 31: 2463.

[5] Obara T, Kobayashi T, Ohyagi S. (2012). Mechanism of deflagration-to-detonation transitions above repeated obstacles. Shock Waves. 22: 627.

[6] Gamezo VN, Ogawa T, Oran ES. (2008). Flame acceleration and DDT in channels with obstacles: Effect of obstacle spacing. Combust. Flame 155: 302.

[7] Oran ES. (2015). From catastrophic accidents to the creation of the universe. Proc. Combust. Inst. 35: 1.

[8] Roy GD, Frolov SM, Borisov AA, Netzer DW. (2004). Pulse detonation propulsion: challenges, current status, and future perspective. Prog. Energ. Combust. 30: 545.

[9] Maeda S, Minami S, Okamoto D, Obara T. (2016). Visualization of deflagration-to-detonation transitions in a channel with repeated obstacles using a hydrogen-oxygen mixture. Shock Waves 26: 573.

[10] Goodwin GB, Houim RW, Oran ES. (2016). Shock transition to detonation in channels with obstacles. Proc. Combust. Inst. In press: http://dx.doi.org/10.1016/j.proci.2016.1006.1160.

[11] Goodwin GB, Houim RW, Oran ES. (2016). Effect of decreasing blockage ratio on DDT in small channels with obstacles. Combust. Flame. 173: 16.

[12] Pinos T, Ciccarelli G. (2015). Combustion wave propagation through a bank of cross-flow cylinders. Combust. Flame. 162: 3254.

[13] Ogawa T, Oran ES, Gamezo VN. (2013). Numerical study on flame acceleration and DDT in an inclined array of cylinders using an AMR technique. Comput. Fluids 85: 63.

[14] Ogawa T, Gamezo VN, Oran ES. (2013). Flame acceleration and transition to detonation in an array of square obstacles. J. Loss Prevent. Proc. 26: 355.

[15] Ciccarelli G, Johansen C, Parravani M. (2011). Transition in the propagation mechanism during flame acceleration in porous media. Proc. Combust. Inst. 33: 2273.

[16] Chao J, Lee JHS. (2003). The propagation mechanism of high speed turbulent deflagrations. Shock Waves 12: 277.

[17] Ogawa T, Gamezo VN, Oran ES (2011). Flame acceleration and transition to detonation in an array of cylinders. in 23rd International Colloquium on the Dynamics of Explosions and Reactive Systems (Irvine, USA).

[18] Houim RW, Kuo KK. (2011). A low-dissipation and time-accurate method for compressible multi-component flow with variable specific heat ratios. J. Comput. Phys. 230: 8527.

[19] Xiao H, Houim RW, Oran ES. (2015). Formation and evolution of distorted tulip flames. Combust. Flame. 162: 4084.

[20] Center for Computational Sciences and Engineering, University of California, Berkeley. (2015). Boxlib. Data Retrieved in December 2015.

[21] Chaudhuri A, Hadjadj A, Chinnayya A. (2011). On the use of immersed boundary methods for shock/obstacle interactions. J. Comput. Phys. 230: 1731.